GA–A28114

MICROWAVE IMAGING REFLECTOMETRY (MIR) FOR THE STUDY OF EDGE HARMONIC OSCILLATIONS (EHOs) ON DIII-D

by
X. REN, M. CHEN, X. CHEN, C.W. DOMIER, N.M. FERRARO, G.J. KRAMER, N.C. LUHMANN, JR., C.M. MUSCATELLO, R. NAZIKIAN, L. SHI, B.J. TOBIAS, AND E. VALEO

JUNE 2015

GENERAL ATOMICS

DISCLAIMER

This report was prepared as an account of work sponsored by an agency of the United States Government. Neither the United States Government nor any agency thereof, nor any of their employees, makes any warranty, express or implied, or assumes any legal liability or responsibility for the accuracy, completeness, or usefulness of any information, apparatus, product, or process disclosed, or represents that its use would not infringe privately owned rights. Reference herein to any specific commercial product, process, or service by trade name, trademark, manufacturer, or otherwise, does not necessarily constitute or imply its endorsement, recommendation, or favoring by the United States Government or any agency thereof. The views and opinions of authors expressed herein do not necessarily state or reflect those of the United States Government or any agency thereof.

GA–A28114

MICROWAVE IMAGING REFLECTOMETRY (MIR) FOR THE STUDY OF EDGE HARMONIC OSCILLATIONS (EHOs) ON DIII-D

by
X. REN[1], M. CHEN[1], X. CHEN[2], C.W. DOMIER[1], N.M. FERRARO[2], G.J. KRAMER[3], N.C. LUHMANN, JR.[1], C.M. MUSCATELLO[1,2], R. NAZIKIAN[3], L. SHI[3], B.J. TOBIAS[3], AND E. VALEO[3]

This is a preprint of a paper to be presented at the First EPS Conference on Plasma Diagnostics, April 14-17, 2015 in Frascati, Italy and to be published in the *Proceedings of Science (POS).*

[1]University of California, Davis, Davis, California, USA
[2]General Atomics, P.O. Box 85606, San Diego, California, USA
[3]Princeton Plasma Physics Laboratory, Princeton, New Jersey, USA

Work supported by
the U.S. Department of Energy under
DE-FG02-99ER54531, DE-FC02-04ER54698, and DE-AC02-09CH11466

GENERAL ATOMICS PROJECT 30200
JUNE 2015

GENERAL ATOMICS

REVIEW SHEET FOR REPORTS, PAPERS, ARTICLES & WEB PUBLICATIONS

GA 752 (REV. 0701 E)

Title	Date	Report No. or Other Identification
Microwave Imaging Reflectometry (MIR) for the study of Edge Harmonic Oscillations (EHOs) on DIII-D	5/4/15	A28114

Author(s)	Org. No.	Ext.	Contract No.	Funding Proj. & W.O. No.
X. Ren et al	495		DE-FC02-04ER54698	B30200.0530

PURPOSE

REPORT

☐ Progress ☒ Topical ☐ Other

TYPE OF REVIEW:

☐ Commitment Authorization

☐ Abstract Approval

☒ Full Text Approval

PAPER/ARTICLE/WEB PUBLICATION

USE:

☐ To be Presented by Author

At 1st EPS Conference on Plasma Diagnostics

Location (City, State/Country) Frascati, Italy Date April 14-17,2015

Meeting Name & Sponsor

☒ To be Submitted for Publication in Proceedings of Science (POS)

☐ Web Publication

☐ Oral Presentation Only (No External Publication or Distribution)

POSSIBLE DISCLOSURE OF INVENTIONS [To be Completed & Initialed by the Author(s) CCP]

NEW* CONCEPTS, IDEAS OR IMPROVEMENTS DISCLOSED BY THIS DOCUMENT Brief Description	Page(s) Where Disclosed	Significance of Technological Advancement over Prior Art
1		☐ Large ☐ Slight ☐ Moderate ☒ None
2		☐ Large ☐ Slight ☐ Moderate ☐ None

*Unless otherwise advised by the Patent Group, "new" means not described in a printed publication that is more than one year old. If document describes no new concept, idea or improvement, enter "none" in block 1. If any invention disclosure(s) has been or will be filed, so indicate.

PRIVATE DATA AND PROPRIETARY INFORMATION [To be Completed by Author(s) CCP]

Will GA Private Data or Proprietary Information be disclosed by the publication of this document? ☐ Yes ☒ No. If yes, the subject document must contain an appropriate legend restricting the use and further disclosure by the recipients. Indicate whether an effort has been made ☐, has not been made ☐, to minimize to the greatest possible extent the disclosure of GA Private Data and Proprietary Information. Approval below by Division Director and Vice President required to release Private Data or Proprietary Information.

EXPORT CONTROLLED INFORMATION [To be Completed by Author(s) CCP]

Will publication/presentation disclose information considered sensitive or critical data that is not publicly available? ☐ Yes ☒ No. If yes, the subject report/paper/article must contain an export control legend restricting the use, further disclosure, and export by the recipients. Will publication/presentation disclose information to foreign persons, inside or outside the U.S. that is not available to the public? ☐ Yes ☒ No. If yes, Export Licensing (LSNC) approval must be obtained below; an export license may be required.

APPROVALS	Signature	Date	Comments
Technical C.C. Petty	CCP	6/16/15	
Division Director R.J. Buttery	RJB	6/15/15	
Program or Project			
Intellectual Properties X2363 C. Langer Patent Clearance Required? ☐ Yes ☐ No			
Contracts R.J. Gompper Customer Approval Reqd.? ☐ Yes ☐ No Restrictive Legend Reqd.? ☐ Yes ☐ No			
Export Licensing (LSNC) X2823 Export Control Approval Req'd? ☐ Yes ☐ No	Rec'd 6/17		
Vice President M.R. Wade		6/17/15	A few things to fix / Done

(Review Sheet original to Document Center/ Copy Distribution: Contracts, Author, Intellectual Properties

When complete, please return to Adele Williams x 3075 ~~13-183~~ 13-109

Microwave Imaging Reflectometry for the study of Edge Harmonic Oscillations on DIII-D*

X. Ren [a,*], M. Chen [a], X. Chen [b], C. W. Domier [a], N. M. Ferraro [b], G. J. Kramer [c], N. C. Luhmann, Jr. [a], Jr., C. M. Muscatello [a,b], R. Nazikian [c], L. Shi [c], B. J. Tobias[c], and E. Valeo[c]

[a] *University of California at Davis,*
1 shield Avenue, Davis, CA, USA, 95616
[b] *General Atomics*
3483 Dunhill St, San Diego, CA, USA 92121
E-mail: xren@ucdavis.edu
[c] *Princeton Plasma Physics Laboratory,*
100 Stellarator Rd., Princeton, NJ, USA 08540

ABSTRACT: Quiescent H-mode (QH) is an ELM free mode of operation in which edge-localized harmonic oscillations (EHOs) are believed to enhance particle transport, thereby stabilizing ELMs and preventing damage to the divertor and plasma facing components. Microwave Imaging Reflectometer (MIR) enabling direct comparison between the measured and simulated 2D images of density fluctuations near the edge can determine the 2D structure of density oscillation which can help to explain the physics behind EHO modes. MIR data sometimes indicates a counter-propagation between higher (n>1) and dominant (n=1) harmonics of coherent EHOs in the steep gradient regions of the pedestal. To preclude diagnostic artifacts, we have performed forward modeling that includes possible optical misalignments to show that offsets between transmitting and receiving antennas do not account for this feature. We have also simulated the non-uniform rotation of the EHO structure, which induces multiple harmonics that are properly characterized in the synthetic diagnostic. Excluding these possible explanations for the data, the counter-propagation observed in MIR data, which is not corroborated by external Mirnov coil array measurements, may be due to subtleties of the eigenmode structure, such as an inversion radius consistent with a magnetic island. Similar effects are observed in analysis of internal ECE-Imaging and BES data. The identification of a non-ideal structure motivates further exploration of nonlinear models of this instability.

KEYWORDS: QH-mode; EHO; MIR; MIR artifact; FWR.

Contents

1. Introduction 1

2. Forward modelling of MIR 2

3. Forward modeling of instrumental non-idealities 3

4. Summary and Future work 7

5. Acknowledgements 8

6. References 8

1. Introduction

Quiescent H-mode [1-3] is one possible operation mode for future fusion reactors, such as ITER. It preserves superior energy confinement while also preventing damage to divertor and other plasma facing components by avoiding ELMs. Edge Harmonic Oscillations (EHOs) [4-7] are believed to be the key element of QH-mode, enhancing particle transport at the edge and allowing the edge plasma to reach equilibrium below the ELM stability boundary. Figure 1 shows an example (DIII-D shot # 157102) of QH-mode without ELMs versus a typical H-mode (DIII-D shot # 154412) with strong ELMs. Recent theory predicts that EHO is a low-n peeling mode with its stability closely tied to toroidal rotation shear [2,3].

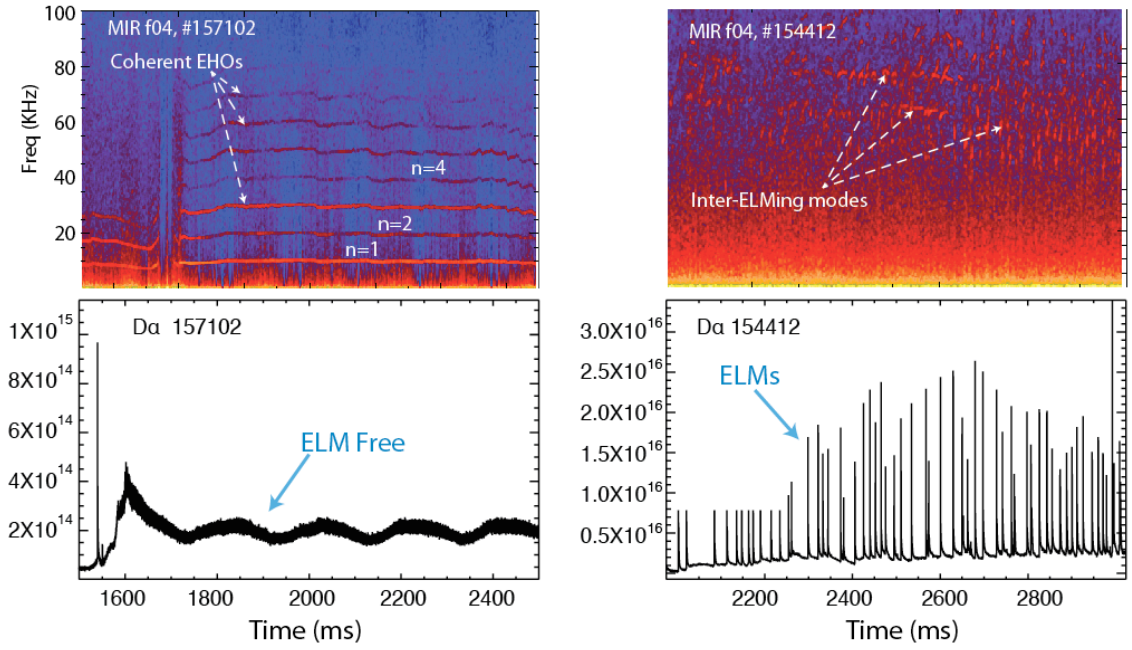

Figure 1: Examples of quiescent H-mode (left) and conventional H-mode (right). The quiescent H-mode has strong coherent EHOs measured with MIR (upper left), and no bursts of Dα radiation at the divertor (lower left). The conventional H-mode is ELMing with frequent spikes of Dα emission (lower right). MIR measured inter-ELMing modes has higher frequencies (upper right) for conventional H-mode.

The Microwave Imaging Reflectometer (MIR) [8-10] on DIII-D is an X-mode imaging reflectometer, with tunable frequency range from 56 to 74 GHz and 20 cm poloidal coverage. MIR is well suited for measuring density fluctuations in the steep gradient pedestal region of H-mode and has been used to compare the poloidal wavenumber spectra of both the coherent and so-called broadband EHO types. These measurements could help to validate a model for EHO excitation and control, as MIR data often exhibits unique features when compared to other diagnostics. Apparent counter propagation is observed in MIR data when imaging near the top of the pedestal. However, this is not reflected in Mirnov coil array data. Figure 2 shows MIR measurements from two frequency/radial channels for discharge # 157102, which is configured with normal Bt, reversed Ip, and counter-current neutral beam torque. Both the dominant mode (n=1) and harmonics (n=2 and n=3) diagnosed with the 57 GHz channel propagate in the same direction to the toroidal torque, which is consistent with Mirnov coil array (an external measurement) data. However, density fluctuation data from the 58 GHz channel, which is located more near the top of pedestal, shows that the dominant mode propagates counter to that measured from the 57 GHz channel, while the other harmonics still co-propagates with the toroidal torque. This is inconsistent with the Mirnov coil array data. Possible sources of instrumental artifacts are investigated using forwarding modeling of MIR; however, they do not reproduce the observed effect of counter-propagating harmonic behavior, leading us to conclude that they are in fact due to subtleties of the EHO mode structure.

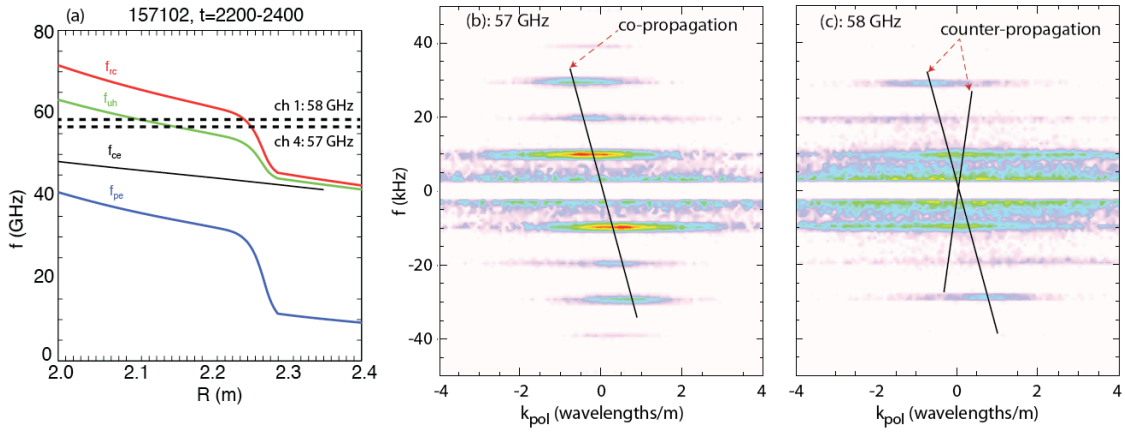

Figure 2: Apparent counter propagation in MIR data. The dominant mode and harmonics measured with the 57 GHz channel (b) are propagating in the same direction, consistent with Mirnov coil array data. However, data from the 58 GHz channel (c), located more near the top of pedestal, measures the dominant mode (n=1) counter propagating with higher harmonics (n=3, etc.).

2. Forward modelling of MIR

The synthetic MIR [11] diagnostic provides a powerful tool to accurately simulate the output of the diagnostic, thus, helping to interpret instabilities and is employed to investigate optical arrangements and possible instrumental artifacts. This forward modeling of MIR is realized with the combination of three components: plasma target with turbulence, full-wave reflection codes FWR [12,13] and MIR optics. The plasma target could be simulation output, or equilibrium profile with experimentally measured edge perturbations. The FWR codes are used to simulate sub-THz wave interaction with the prescribed plasma. FWR-2D code calculates reflection in the poloidal plane and is well established and extensively used; while the 3D code calculates reflection over a 3D volume and is to simultaneously provide electron density and temperature perturbation. Simulation results from FWR2D, due to its better stability, are presented in the following content. The beam field applied in FWR is generated from diffraction modeling of the MIR optics employing beamlet-based wave propagations.

The method of generating synthetic diagnostic signals from plasma simulation output is illustrated in Fig. 3 below. A time-series (or periodic sequence) of perturbed field data from simulation is combined with the optical field patterns of the diagnostic to produce time-dependent synthetic imaging data. Thousands of time-points can be generated with the usage of an efficient algorithm of the full-wave reflection code FWR2D, which utilizes a very efficient paraxial-wave solution to solve for propagation in regions far from the cutoff but within the large (a/λ) plasma volume of DIII-D. The reflected field from FWR is combined with the MIR receiver beam field to produce a synthetic diagnostic signal, resolving phase/density fluctuations on the cutoff layer. Synthetic imaging data may be analyzed by the same methods applied to real data on DIII-D in order to understand the diagnostic response and features of the visualization.

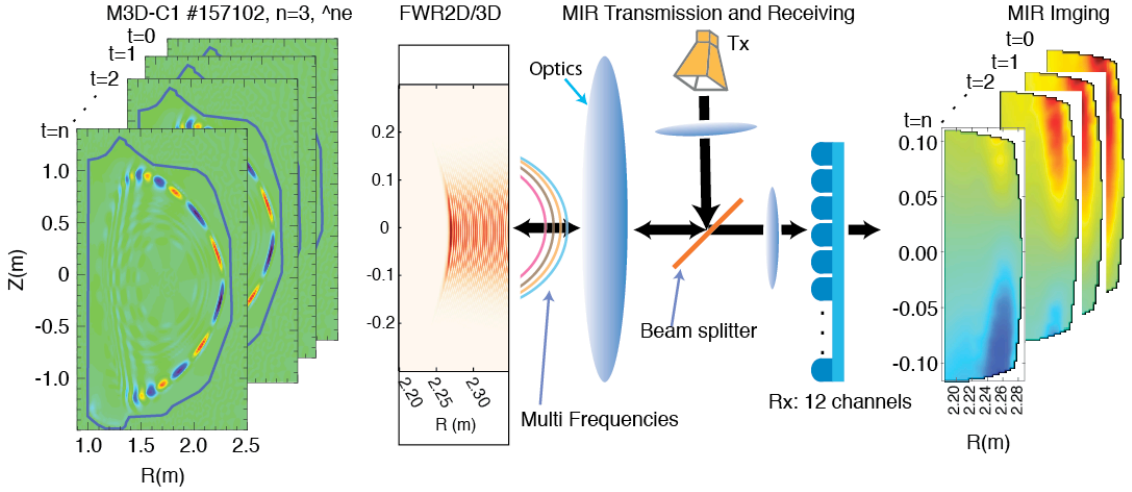

Figure 3: The process of forward modeling MIR diagnostic output from the 3D MHD code M3D-C1. Time-dependent output from M3D-C1 has been provided for shot # 157102 with the n=3, 5 coherent EHO mode. These are inserted as perturbed fields into the simulation domain of FWR. Antenna patterns taken from the diffractive modeling of MIR imaging optics are used as boundary conditions for the simulation. The converged electric field pattern at the outgoing

microwave boundary is taken at each time step of the simulation and compared with the receiver antenna pattern to produce a quadrature (amplitude and phase) signal time point.

3. Forward modeling of instrumental non-idealities

Examples of synthetic images produced by the synthetic diagnostic are given in Figure 4, with the upper row representing forward modeling results, and the lower row representing plasma simulation output results. Probing frequencies range from 55 to 61 GHz with 1 GHz intervals, and cover the top pedestal region where the peak of the fluctuation amplitude resides. There are 12 poloidally evenly spaced channels in each frequency/density channel with resolution of approximately 3.0 cm. Note that the poloidal coverage is only 20 cm, much less than the wavelength of the most destabilized coherent EHO modes (n<=5), making it challenging to resolve the long wavelengths (k_{pol} ~ 0.1/cm). The 3D MHD code M3D-C1 [14,15] is being used to model the QH-mode on DIII-D with the presence of a low-n (≤5) EHO mode. M3D-C1 does not obtain a saturated n=1 or n=2 mode for shot # 157102; thus, the destabilized higher modes n=3 and n=5 are applied. As shown on Fig. 4, by scaling the phase of the reflectometer signal (upper row) appropriately with the density perturbation displacement (lower row), the two sequences are nearly indistinguishable, indicating that the forward modeling accurately resolved the input density fluctuations. The peak density fluctuation associated with the coherent EHO fluctuation from M3D-C1 simulation is located at 2.26 m, while the measured maximum fluctuation in the synthetic MIR signal is at 2.258 m, with only 2 mm difference. This difference is due to the fact that the peaked fluctuation is located between two probed cutoff layers.

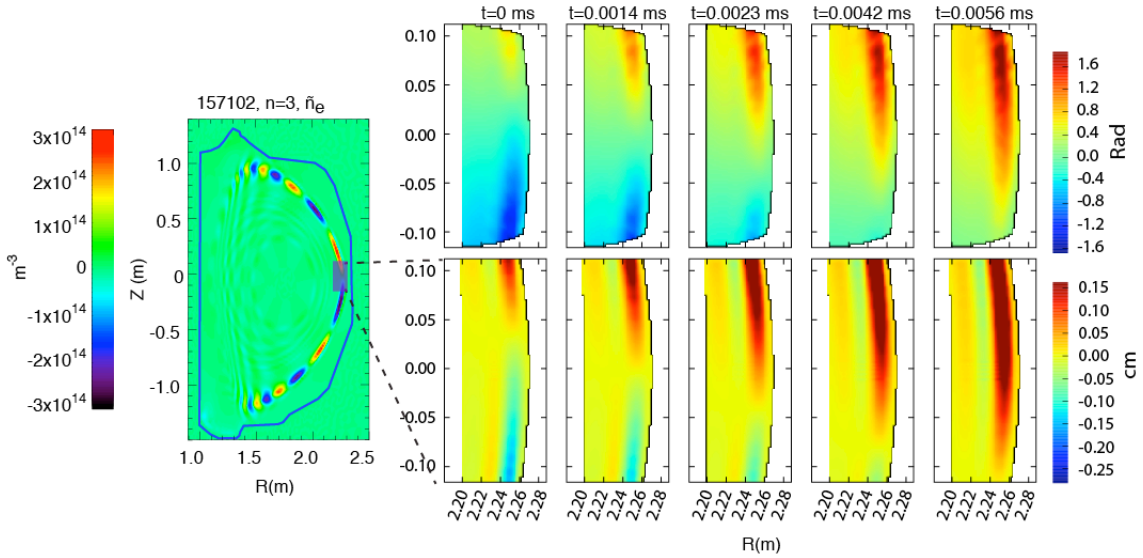

Figure 4: Synthetic images of phase perturbation produced by synthetic diagnostic (upper row) and images of density perturbation displacement from M3D-C1 simulation output (lower row). The n=3 electron density fluctuation produced by M3D-C1 is shown at left. This perturbation is evolved in time to produce the images in the top row from an idealized MIR diagnostic with 6 probing frequencies. The perturbation on the upper row is nearly indistinguishable with the lower row with scaled phase and displacement perturbation.

Since the counter propagation observed in MIR data measured near the top of pedestal could be due to either imperfections of the instrument, or subtleties of the eigenmode structure,

instrument imperfections as well as partial non-uniform rotation of coherent EHO are investigated with three different forward modeling setups: linear EHO modes with ideal MIR optics, linear EHO modes with mis-aligned MIR optics, and nonlinear EHO mode with ideal MIR optics.

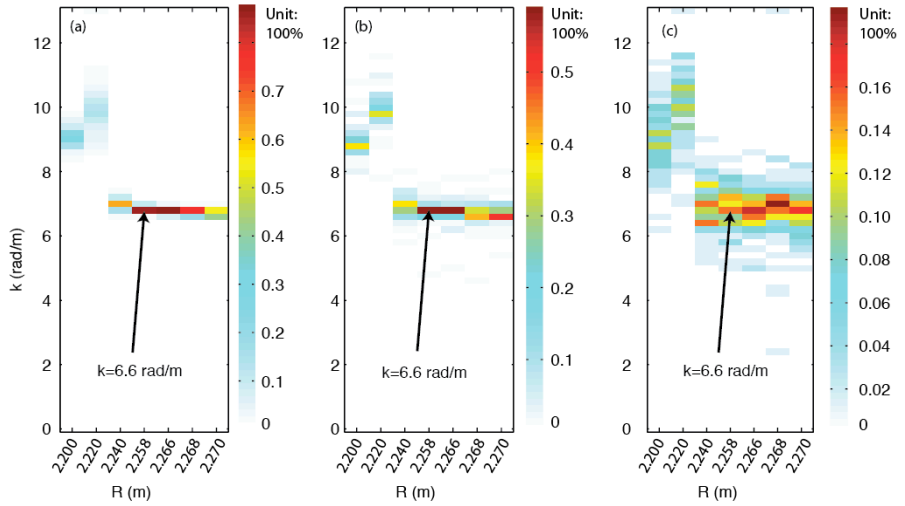

Figure 5: Wavenumber distribution along the radial direction obtained from (a) M3D-C1 output, (b) forward modeling output with ideal optical alignment and (c) forward modeling output with mis-aligned optics. This measurement becomes less certain when modest optical misalignments are introduced, but the peak of the distribution remains centered on the correct wavenumber.

Linear EHO n=3 and n=5 modes located near the edge, are destabilized within M3D-C1 simulations, and with their fluctuation amplitude increased to the experimental level (around 5.2 mm maximum radial perturbation, one free space wavelength of probing wave) are measured with MIR forward modeling with and without optical misalignment. Figure 5 shows the wavenumber distribution over each frequency/radial channel for mode n=3. The two most inside radial channels, with smallest fluctuation amplitude, show different wavenumbers to the other edge channels, and this is due to some subtleties in their mode structure. Since these two channels are well inside the pedestal region where dominant EHO is located, this unforeseen difference in wavenumber from simulation is reasonable. Figure 5 (c) shows the wavenumber distribution when transmitter and receiver are mis-aligned by 4 cm vertically. Compared to the case when receiver and transmitter in Fig. 5 (b) are well aligned, the wavenumber seems distributed more widely, while the peak value of the wavenumber is still measured correctly.

The forward modeling results shown in Fig. (5) suggest that vertical offset between transmitting and receiver antennas doesn't account for the apparent counter-propagation. Both M3D-C1 output and forward modeling yield center wavenumber k around 6.6 rad/m for n=3. The experimental measurement of the wavenumber for the dominant n=1 mode is 2.5 rad/m, which is around 1/3 times of that of n=3. This means the n=3 mode has similar phase velocity as that of the n=1 mode. However, experimental measurement of the n=3 EHO component gives a local poloidal wavenumber of ~ 3.14 rad/m, which is less than that predicted by the forward modeling of M3D-C1 data. This uncertainty as well as observed counter-propagation may be due to the non-sinusoidal nature of the density fluctuation in experiment, which is not inherent

to the M3D-C1 result. This has been partially explored by varying the time dependence of the oscillation of linear EHO mode. The magnetic flux displacement obtained from M3D-C1 output is nearly:

$$d(x,t)=a_0\cos(\omega t+\Delta\Phi(x)) \quad \text{with} \quad \Delta\Phi(x)=kx+\varphi_0$$

Higher fluctuation components, with their amplitudes less than half of that of the dominant n=3 component, are added to manipulate the mode structure:

$$d(x,t)=a_0\cos(\omega t+\Delta\Phi(x))+a_1\cos(2*\omega t+2*\Delta\Phi(x))$$
$$+a_2\cos(3*\omega t+3*\Delta\Phi(x))+\cdots+a_6\cos(7*\omega t+7*\Delta\Phi(x))$$

with

$$a_0\geq 2*a_1\geq\cdots\geq 2^6*a_6$$

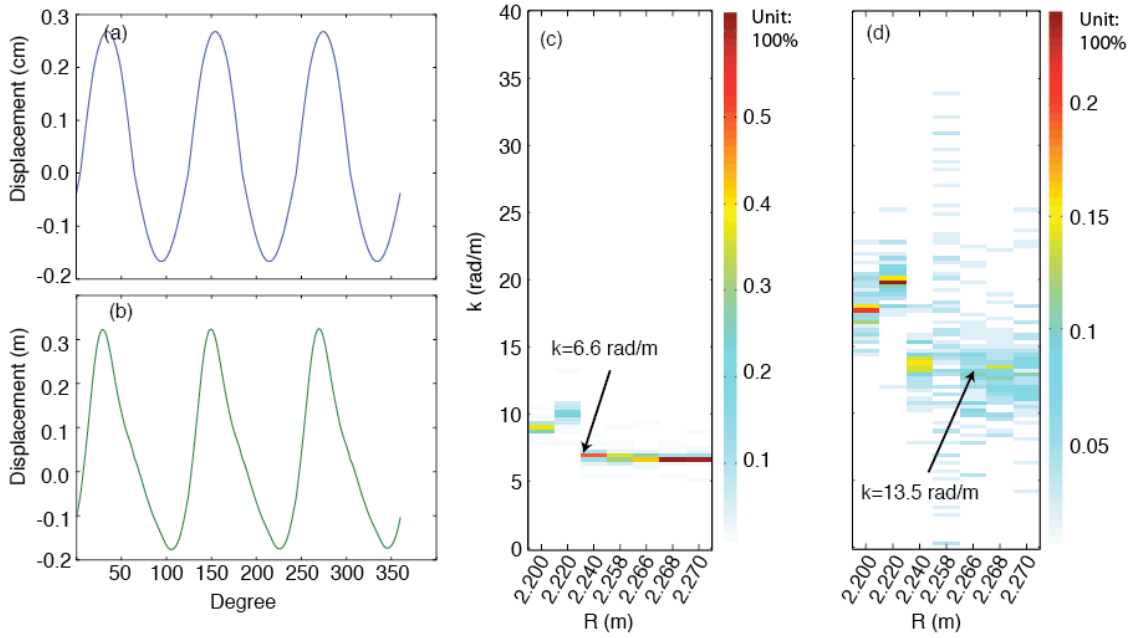

Figure 6: Wavenumber distributions of linear (a) and nonlinear (b) time-dependent fluctuations. (c) and (d) shows the corresponding wavenumber distribution from forward modeling for the dominant and 2nd harmonic of n=3, while both yield the correct center wavenumber.

Figure 6 (a) and (b) shows the mode structure for both linear/sinusoidal and nonlinear/non-sinusoidal perturbations. Forward modeling measurements for the non-sinusoidal suggest that harmonic wavenumber can still be diagnosed correctly, as highlighted in Figs. 6 (c) and (d). This result suggests that the non-uniform rotation of EHO mode is not the source of the counter-propagation. Since the experimental fluctuation has a dominant mode number of n=1, which is not destabilized with M3D-C1 simulations for shot 157102, more realistic mode structures are needed to eliminate non-linearity as a reason for counter-propagation. Further exploration with FWR3D is warranted determine the remaining uncertainties.

Since the forwarding modeling indicates that neither misalignment between the transmitting and receiving antennas nor non-uniform rotation of the EHO can account for the measured counter propagation, we are led to speculate as to whether the counter propagation is a similar diagnostic artifact as seen in ECEI data [16], which is known to correspond with a flucutation phase inversion due to magnetic islands. This weak tearing parity has been overlooked in the past, but a similar feature has now been observed in BES and other ECE data, as shown in Fig. 7. The MIR artifact signal may be due to the similar phase inversion in density fluctuations caused by EHO near the top of pedestal.

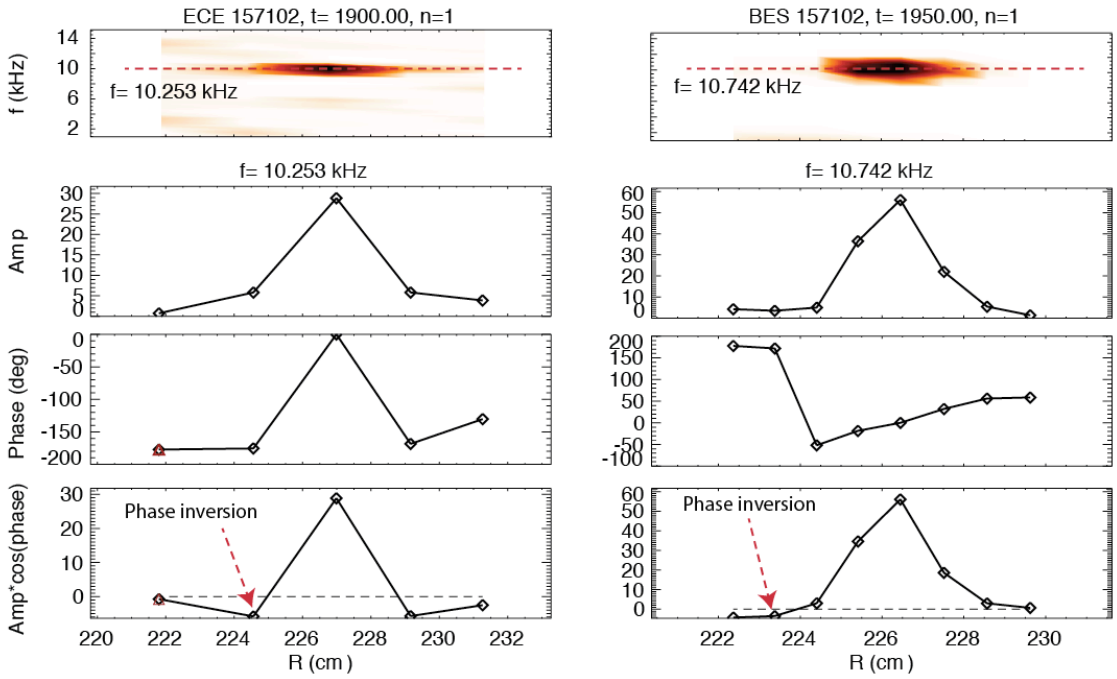

Figure 7: Phase inversion observed in both ECE and BES data. As the coherent EHO mode (n=1) decreasing towards into plasma, before its disappearance, an obvious phase inversion is captured for shot # 157102, and the similar reason could cause the counter-propagation seen in MIR data.

4. Summary and future work

MIR on DIII-D measures detailed characteristics about EHO, and helps to explain how EHO modes are destabilized, how they saturate, and by what mechanisms they limit the evolution of the H-mode pedestal, while inconsistency measurements, say counter propagation, also suggests instrumental imperfections. Both optical mis-alignment and non-uniform EHO rotation are investigated as possible instrumental artifact sources using the forwarding modeling of MIR, but they do not reproduce the observed effects of counter propagating harmonic behaviors. Excluding these possible explanations, the apparent counter-rotation of the mode structure near the top of the pedestal could in fact be a diagnostic artificial due to phase/radius inversion of the EHO of that location that is consistent with observations from ECE-Imaging and BES. More sophisticated, nonlinear models, applying both FWR2D and more advanced FWR3D will be applied to explore remaining uncertainties.

Acknowledgments

*This work is supported by US DOE grants DE-AC02-09CH11466, DE-FG02-99ER54531, DE-FC02-04ER54698 and DE-SC0012551.

References

[1] K. H. Burrell, et al., *Quiescent H-mode plasmas in the DIII-D tokamak*, Plasma Phys. and Controll. Fusion 44, A253 (2002)

[2] K. H. Burrell, et al., *Edge pedestal control in quiescent H-mode discharges in DIII-D using co-plus counter-neutral beam injection*, Nucl. Fusion 49, 085024 (2009)

[3] K. H. Burrell, et al., *Quiescent H-Mode Plasmas with Strong Edge Rotation in the Cocurrent Direction*, Phys. Rev. Lett. 102, 155003 (2009)

[4] A. M. Garofalo, et al., *Advances towards QH-mode viability for ELM-stable operation in ITER*, Nucl. Fusion 51(2011),083018 (10pp)

[5] L. J. Zheng, et.al. *Low-n magnetohydrodynamic edge instabilities in quiescent H-mode plasmas with a safety-factor plateau*, Nucl. Fusion 53 (2013) 063009 (9pp)

[6] L. Zeng, et al., *Dynamic of pedestal perturbations by ELMs and edge harmonic oscillations in DIII-D*, Plasma Phys. Control. Fusion 46 (2004) A121-A129

[7] Z. Yan, et al., *High-Frequency Coherent Edge Fluctuations in a High-Pedestal-Pressure Quiescent H-Mode Plasma*, Phys. Rev. Lett. 107,055004 (2011)

[8] C. M. Muscatello, et al., *Technical overview of the millimeter-wave imaging reflectometer on the DIII-D tokamak*, Rev. Sci. Instrum. 85, 11D702 (2014)

[9] C. M. Muscatello, et al., *Multi-dimensional visualization of turbulence in fusion plasmas*, IEEE Transactions on Plasma Science 42, 2734 (2014)

[10] A. G. Spear, et al., *2D microwave imaging reflectometer electronics*, Rev. Sci. Instrum. 85, 2014

[11] X. Ren, et al., *Process to generate a synthetic diagnostic for microwave imaging reflectometry with the full-wave code FWR2D*, Rev. Sci. Instrum. 85, 11D863 (2014)

[12] E. J. Valeo, G. J. Kramer, R. Nazikian, *Two-dimensional simulations of correlation reflectometry in fusion plasmas*, Plasma Phys. and Control. Fusion 44, L1 (2002)

[13] G. J. Kramer, R. Nazikian, and E. Valeo, *Effects of two-dimensional and finite density fluctuations on O-X correlation reflectometry*, Plasma Phys. Controlled Fusion 44, L11 (2002)

[14] N. M. Ferrara, et al., *Calculations of two-fluid magnetohydrodynamic axisymmetric steady-states*, Journal of Computational Physics 228(20), pp 7742-7770, (2009)

[15] S. C. Jardin, et al., "The M3D-C1 approach to simulating 2-fluid magnetohydrodynamics in magnetic fusion experiments", Journal of Physics: Conference Series 125, 012044 (2008)

[16] B. Tobias, et al., *Phase-locking of magnetic islands diagnosed by ECE-imaging*, Rev. Sci. Instrum. 85, 11D847 (2014)